# Spatial variations in larch needle and soil $\delta^{15}N$ at a forest-grassland boundary in northern Mongolia

Lei Fujiyoshi[1], Atsuko Sugimoto[1, 2, 3*], Akemi Tsukuura[1], Asami Kitayama[1], M. Larry Lopez Caceres[4], Byambasuren Mijidsuren[5], Ariunaa Saraadanzar[5], Maki Tsujimura[6]

[1]*Graduate School of Environmental Science, Hokkaido University, Sapporo, Hokkaido 060-0810, Japan*

*Phone: +81-(0)11-706-2233*

[2]*Faculty of Environmental Earth Science, Hokkaido University, Sapporo, Hokkaido 060-0810, Japan*

*Phone: +81-(0)11-706-2233*

[3]*Arctic Research Center, Hokkaido University, Sapporo, Hokkaido 001-0021, Japan*

*Phone: +81-(0)11-706-9075*

[4]*Faculty of Agriculture, Yamagata University, Tsuruoka, Yamagata 997-8555, Japan*

*Phone: +81-(0)23-528-2805*

[5]*Plant Protection Research Institute, Mongolian University of Life Sciences, Zaisan 210153, Ulaanbaatar, Mongolia*

*Phone: +976-11-345212*

[6]*Faculty of Life and Environmental Sciences, University of Tsukuba, Tsukuba, Ibaraki 305-8572, Japan*

*Phone: +81-(0)29-853-2568*

e-mail:

Lei Fujiyoshi (green-nandin@ees.hokucai.ac.jp), *Atsuko Sugimoto (sugimoto@star.dti2.ne.jp), Akemi Tsukuura (akemi.tsukuura@gmail.com), Asami Kitayama (asami.kitayama@ees.hokudai.ac.jp), M. Larry Lopez Caceres (larry@tds1.tr.yamagata-u.ac.jp), Byambasuren Mijidsuren (byamba0730@yahoo.com), Ariunaa Saraadanzar (ardiu99@yahoo.com), Maki Tsujimura (mktsuji@geoenv.tsukuba.ac.jp)

*Correspondence to: Atsuko Sugimoto (sugimoto@star.dti2.ne.jp)

*Acknowledgement*

This study was partly supported by the Japan Society for the Promotion of Science with a Grant-in-Aid for Scientific Research (No. 26281003).

# Spatial variations in larch needle and soil $\delta^{15}N$ at a forest-grassland boundary in northern Mongolia

The spatial patterns of plant and soil $\delta^{15}N$ and associated processes in the N cycle were investigated at a forest-grassland boundary in northern Mongolia. Needles of *Larix sibirica* Ledeb. and soils collected from two study areas were analysed to calculate the differences in $\delta^{15}N$ between needle and soil ($\Delta\delta^{15}N$). $\Delta\delta^{15}N$ showed a clear variation, ranging from -8‰ in the forest to -2‰ in the grassland boundary, and corresponded to the accumulation of organic layer. In the forest, the separation of available N produced in the soil with $^{15}N$-depleted N uptake by larch and $^{15}N$-enriched N immobilization by microorganisms was proposed to cause large $\Delta\delta^{15}N$, whereas in the grassland boundary, small $\Delta\delta^{15}N$ was explained by the transport of the most available N into larch. The divergence of available N between larch and microorganisms in the soil, and the accumulation of diverged N in the organic layer control the variation in $\Delta\delta^{15}N$.

Keywords: nitrogen isotope ratio; larch; soil; forest-grassland boundary; Mongolia; organic layer

54

55 ## 1. Introduction

56 Nitrogen (N) is one of the key elements in biological processes. The N cycle in
57 plant-soil system includes the decomposition of soil organic matter, the uptake of
58 biologically available N (e.g. $NH_4^+$ and $NO_3^-$) by plants and soil microorganisms, and
59 the return of litterfall to the soil as an internal processes, as well the N input as
60 atmospheric deposition and/or biological $N_2$ fixation, and the loss by leaching and/or
61 gaseous emission as external processes [1]. All these processes result in variations in
62 plant and soil $\delta^{15}N$, which are caused by differences in the $\delta^{15}N$ of sources for plants [2],
63 N loss, such as nitrate ($NO_3^-$) leaching [3] or gaseous emission ($N_2O$, $N_2$) via
64 nitrification and denitrification [4], decomposition processes, such as mineralization and
65 nitrification[5], mycorrhizal fungi [6], and physiological processes within the plant [7].
66 As a result, plant and soil $\delta^{15}N$ serve as useful indicators of the N cycle in the plant-soil
67 system [8].

68 The $\delta^{15}N$ values of plant and soil in forest ecosystem have been investigated and
69 various characteristics have been reported [9]. The plant $\delta^{15}N$ values of co-occurring
70 species in boreal forest showed differences among species, which were attributed to the
71 different N source for each species in terms of N form and/or the depth of N uptake [10].

On the other hand, it has been shown that soil $\delta^{15}N$ generally increases with depth, from organic layer which is typically observed in forest, to mineral soil [11]. Previous studies also showed that the organic layer contributes as significant nitrogen source for trees [12, 13]. Furthermore, recent global syntheses in $\delta^{15}N$ values have shown the spatial trends in $\delta^{15}N$ values of plant and soil along climate gradient [14–16].

The difference between plant and soil $\delta^{15}N$ ($\Delta\delta^{15}N$ = plant $\delta^{15}N$ - soil $\delta^{15}N$), which is an apparent enrichment factor, allows the comparison of different sites by normalizing the spatial heterogeneity in soil $\delta^{15}N$ [17].$\Delta\delta^{15}N$ has been widely applied, and variations in $\Delta\delta^{15}N$ have been attributed to various causes such as differences in N forms that plant uptake (DON, $NH_4^+$, or $NO_3^-$) [17–22] and changes in $\delta^{15}N$ of each N form affected by nitrification [17,18,23,24]. Mycorrhizal fungi have also been reported to affect $\delta^{15}N$ through $^{15}N$-enrichment in the fungal body [25], although the degree of enrichment is still controversial [26]. Not only these internal processes within the plant-soil system, but also atmospheric N deposition that serve as the N source for plants [27], has been reported to cause variations in $\Delta\delta^{15}N$. Additionally, the strategy of field observations often complicates the interpretation of $\Delta\delta^{15}N$. Previous studies set wide spatial scales (region, country, or globe) along the gradient of specific environmental variables (climate, topography, soil age, and parent material), which hampered the interpretation

of $\Delta\delta^{15}N$, due to the needed comparison among different plant species with different degrees of isotopic fractionation within the plant body [7], and the co-existence of variables that affect plant and soil $\delta^{15}N$ [14].

In this study, we investigated a forest-grassland boundary (ecotone) ecosystem in northern Mongolia, in which vegetation changes from Siberian larch (*Larix sibirica* Ledeb.) forest to temperate grassland within a very short distance of a few kilometres. Investigation of this ecotone offered the following advantages: (1) existence of a single plant species (*L. sibirica* Ledeb.) that allowed comparisons along the forest-grassland gradient, and (2) exclusion of variables such as climate, soil age, and parent material which were considered similar at all sites within this region. Therefore, this study aimed to clarify the spatial patterns and underlying mechanisms that control $\Delta\delta^{15}N$ which arise only from the differences between forest and grassland ecosystems.

## 2. Materials and methods

### 2.1. *Site description*

Two study areas, Terelj (TR) and Mongonmorit (MM), were chosen for sampling at a forest-grassland boundary in northern Mongolia (Figure 1(a)). Information on site

108 locations and positions is presented in Table 1. The forest consists of Siberian larch
109 (*Larix sibirica* Ledeb.) and white birch (*Betula platyphylla* Sukach.) in some places
110 [28,29]. This region corresponds to the southern boundary of permafrost [29], which
111 coincides with the distribution of boreal forest. The forest dominates the north-facing
112 slopes, whereas temperate grassland dominates the south-facing slopes, dry valleys, and
113 flat plains [29]. The soil in this region is cryosol, and the climate is cold continental
114 climate with dry winters, according to Köppen-Geiger climate classification [30]. The
115 mean annual temperature (MAT) is -3.6°C in TR area and -2.9°C in MM area, and
116 average temperature from May to September is 10.4°C in TR area and 11.2°C in MM
117 area. The mean annual precipitation (MAP) is 353 mm in TR area and 272 mm in MM
118 area, whereas 90% of precipitation occurs during the growing season of larch trees
119 (May to September) [28].
120 In this study, samplings were conducted along the forest-grassland gradient, and the
121 sampling sites were classified as forest or boundary as described by Tuhkanen [31].
122 Forest site was defined as the site in the continuous forest, whereas boundary site was
123 defined as the site between the edge of continuous forest and grassland. In TR area,
124 sampling was conducted along a transect from the north-facing slope to the south-facing
125 slope over a valley at 11 sites (TR1n to TR2s) (Figure 1(b)), whereas in MM area, two

126 transects were set on the south-facing slope and southwest-facing slope and sampling
127 was conducted at 10 sites (MM1sw to MM7s) (Figure 1(c)). Among the 21 sites in total,
128 6 sites in TR area (TR1n to TR6n) and 6 sites in MM area (MM1sw to MM3s) were
129 forest sites, and the rest were boundary sites, except for patchy forest (TR1s) and
130 grassland site with no trees (TR2s) in TR area. Both TR and MM areas included
131 forest-grassland gradient, however MM area had more boundary sites with sparser tree
132 distribution on south-facing slope. Observations at those sites in these two areas covered
133 all range of forest-grassland gradient, and also wide range of conditions regarding
134 organic layer accumulation (litter, fermentation, and humus), which was relatively rich
135 in forest sites (mor-type) to poor in boundary sites (mull-type) [32].
136 [Figure 1 and Table 1 near here]
137

138 **2.2. *Sampling***

139 2.2.1. *Foliar samples*

140 Larch needles were collected during the growing season (May to August) from 2004 to
141 2012. Needles from three to four branches at a height of 1 to 5 m were taken from each
142 tree. More than three trees were usually sampled at each site, but only one or two trees
143 in boundary sites due to their limited number. Needles were also collected from several

144 trees at three sites in TR area (TR3n, TR6n, and TR1s) and two sites in MM area
145 (MM2s and MM1sw) during the growing season of 2004 and 2005 to evaluate temporal
146 variations. Needle samples were oven-dried at 60°C, milled, and wrapped in tin cups for
147 analysis.

148 2.2.2. *Soil samples*

149 Soil samples were collected at the same sites as needle samples. A small pit (0.6 m × 0.6
150 m × 0.6 m deep) was made, and one to three cores (1.5 cm diameter, 4.5 cm length) of
151 bulk soil were collected from the cross section of the pit every 10 cm from 0 cm (the top
152 of mineral soil) down to 50 cm depth or until a rock appeared. The organic layer was
153 also sampled by collecting the organic matter above the mineral soil. The fresh soil
154 samples were sieved with a 2 mm mesh to remove gravel and living roots, oven-dried at
155 105°C for more than 24 h, and used for isotope analysis. Fresh soil samples collected in
156 2012 were also used for KCl-extractable N (DON, $NH_4^+$, and $NO_3^-$) analysis.

157

158 **2.3.** ***Analysis***

159 2.3.1. *C/ N isotopic ratio and concentrations*

160 The $\delta^{13}C$, $\delta^{15}N$, and C, N concentrations were analysed using Conflo system with
161 DELTA V Plus and FlashEA 1112 (Thermo Fisher Scientific) at the Graduate School of

Environmental Science, Hokkaido University, Japan. The isotope ratio was expressed using the δ notation:

$$\delta^{15}N \text{ (or } \delta^{13}C) = \left( \frac{R_{sample}}{R_{std}} - 1 \right) \times 1000 \quad (‰)$$

where $R_{sample}$ is the isotope ratio ($^{13}C/^{12}C$ or $^{15}N/^{14}N$) of a sample, and $R_{std}$ is the isotope ratio ($^{13}C/^{12}C$ or $^{15}N/^{14}N$) of Vienna Pee Dee Belemnite (VPDB) or atmospheric $N_2$ for C and N. Analytical errors were at 0.2‰ for $\delta^{13}C$, 0.3‰ for $\delta^{15}N$, 0.5% for the bulk C concentration, and 0.1% for the bulk N concentration.

2.3.2. *KCl-extractable N*

Soil N pools (DON, $NH_4^+$, and $NO_3^-$) were extracted from 4 g of fresh soil with 40 ml of 2M KCl after 1 h of shaking and filtration. The extracts were kept in coolers, transported to the laboratory, and stored in a freezer until analysis. The concentration of $NO_3^-$, $NH_4^+$, and total dissolved N (TDN) was analysed colorimetrically using a continuous flow nutrient analyser (QuAAtro; BRAN+LUEBBE, Hamburg, Germany). Then, the concentration of dissolved organic N (DON) was calculated by subtracting total inorganic N ($NO_3^-$ and $NH_4^+$) from TDN. The concentration of nitrite ($NO_2^-$) was also analysed, but not detected in any samples.

2.3.3. *Calculation of average values at each site*

To obtain needle N concentration, $\delta^{15}N$, and $\delta^{13}C$ at each site, data were first averaged

180 for all trees in each sampling period excluding those obtained in May, and then
181 averaged for all sampling periods at each site. Needle $\delta^{15}N$, $\delta^{13}C$, and N concentrations
182 observed on all sampling dates at each site are shown in Figure S1. For bulk soil $\delta^{15}N$ at
183 each site, the weighted mean of $\delta^{15}N$ in the 0-20 cm soil layer was calculated from all
184 the available data. The mean N concentration and the C/N ratio in the 0-20 cm soil layer
185 at each site were also calculated from all the available data. $\Delta\delta^{15}N$ was calculated as
186 (needle $\delta^{15}N$ – soil $\delta^{15}N$) at each site.

187 2.3.4. *Isotope mass balance on available N*

188 To interpret the processes reflected in the variation of $\Delta\delta^{15}N$, we applied the mass
189 balance of biologically available N. Assuming that the available N pool is at a steady
190 state, the following equations are established:

191 $$F_{input} + F_a = F_p + F_m + F_{leach} + F_{gas} \quad (1)$$

192 and for $\delta^{15}N$,

193 $$F_{input} \times \delta_{input} + F_a \times \delta_a = F_p \times \delta_p + F_m \times \delta_m + F_{leach} \times \delta_{leach} + F_{gas} \times \delta_{gas} \quad (2)$$

194 where $F_{input}$ is the N derived from atmospheric N deposition and biological $N_2$ fixation,
195 and $F_a$ is the N produced in the soil through the decomposition of soil organic matter. $F_P$
196 and $F_m$ are the fluxes of available N taken up by plants and immobilized by soil
197 microorganisms, respectively. $F_{leach}$ and $F_{gas}$ are the N lost due to leaching and gaseous

198 emission, respectively. The values of $\delta_{input}$, $\delta_a$, $\delta_{p,}$ $\delta_m$, $\delta_{leach}$, and $\delta_{gas}$ are the $\delta^{15}N$ of input,
199 produced N from soil organic matter, plant uptake, immobilization by soil
200 microorganisms, leaching, and gaseous emission of available N, respectively. We
201 assumed that larch was the only plant species (i.e. $\delta_p$ = needle $\delta^{15}N$), and that the $\delta^{15}N$ of
202 available N produced in the soil was the same as that of the soil (i.e. $\delta_a$ = soil $\delta^{15}N$).
203 Generally, available N produced in the soil has similar $\delta^{15}N$ to that of soil organic matter,
204 if all produced N remains in the N pool without any fractionated loss [33]. The
205 schematic representation of each process is shown in Figure S2.

206 2.3.5. *Statistical analysis*

207 The temporal variation of tree components was evaluated by Wilcoxon signed-rank test
208 at $p < 0.05$ (two-tailed). The spatial relationships between the variables were evaluated
209 by Spearman's rank correlation coefficient at $p < 0.05$ (two-tailed).

210

211

212 **3. Results**

213 **3.1. *Temporal variations in $\delta^{15}N$, $\delta^{13}C$, and N concentration of larch needles***

214 Temporal variations in needle N concentration, $\delta^{15}N$, and $\delta^{13}C$ of nine individual trees
215 were observed during the growing season of 2004 and in July 2005 at three sites in TR

area (TR3n, TR6n, and TR1s) (Figure 2). Needle N concentrations were significantly higher in May 2004 than the following months in 2004 and July in 2005 ($p < 0.05$) (Figure 2(a)). Temporal changes or inter-annual variations were not observed for $\delta^{15}N$ and $\delta^{13}C$ (Figure 2(b) and 2(c)). The same temporal variations were also observed in MM area (data not shown). When the data collected in May were excluded, the standard deviations of individual trees during the observed period were 0.4%, 0.5‰, and 0.9‰ for N concentration, $\delta^{15}N$, and $\delta^{13}C$, respectively.

[Figure 2 near here]

### 3.2. *Vertical profile of larch needle, organic layer, and bulk soil $\delta^{15}N$*

The $\delta^{15}N$ value increased vertically from needle, organic layer to soil with depth, and also differed between forest and boundary sites, as seen in the example for TR area (Figure 3). At the forest site (TR1n) and the boundary site (TR7n), soil $\delta^{15}N$ increased up to 20-30 cm soil depth. This pattern in soil $\delta^{15}N$ was common at all sites in TR and MM areas. However, changes in the $\delta^{15}N$ of needle, organic layer, and soil were different between the two sites; a gradual increase in $\delta^{15}N$ was observed at TR1n, whereas a slight increase was observed at TR7n. Similarly, in MM area, a gradual increase in the $\delta^{15}N$ from needle, organic layer to soil was observed at the forest site

234 (MM2sw), whereas slight increase was observed at the boundary sites, especially at
235 MM5s, MM6s and MM7s (data not shown). [Figure 3 near here]
236
237 **3.3.** ***Spatial variations along the forest-grassland gradient***
238 Characteristic spatial patterns in $\delta^{15}N$ values, needle $\delta^{13}C$, and needle N concentration
239 were observed along the forest-grassland gradient in TR and MM areas (Figure 4). In
240 TR area, needle $\delta^{15}N$ increased gradually from -3.9‰ at the forest site (TR1n) to +3.3‰
241 at the boundary site (TR8n) on the north-facing slope, whereas on the south-facing
242 slope, needle $\delta^{15}N$ at TR1s in the patch forest (+1.2‰) was similar to that at TR6n and
243 slightly lower than that at TR8n. In contrast to needle $\delta^{15}N$, soil $\delta^{15}N$ slightly varied
244 from +2.9‰ at TR2n to +5.3‰ at TR7n on the north-facing slope, whereas it was
245 higher on the south-facing slope at TR1s (+5.8‰) and TR2s (+7.4‰). The values of
246 $\Delta\delta^{15}N$ showed the same pattern as needle $\delta^{15}N$ on the north-facing slope (Figure 4(b));
247 $\Delta\delta^{15}N$ was larger in the forest (-8‰ at TR1n) and smaller in the boundary (-3‰ at
248 TR7n) on the north-facing slope, whereas $\Delta\delta^{15}N$ at TR1s on the south-facing slope
249 (-5‰) was similar to that at TR5n. On the north-facing slope, needle $\delta^{13}C$ increased
250 from -27.8‰ to -26.2‰ from the forest site (TR1n) to the boundary site (TR8n), and
251 needle N concentration also increased from 2.0% to 2.7%, respectively. On the

252 south-facing slope, needle $\delta^{13}C$ at TR1s (-26.0‰) was as high as that at TR8n, and
253 needle N concentration at TR1s (2.4%) was similar to that at TR7n (Figure 4(c)).
254 KCl-extractable N (DON, $NH_4^+$, and $NO_3^-$) pools in the 0-20 cm soil layer were
255 observed at two forest sites on the north-facing slope (TR2n and TR5n) in August 2012
256 (Table S1). At both sites, DON was more than one-order of magnitude larger than $NH_4^+$
257 and $NO_3^-$ pools. Additionally, $NH_4^+$ pool was larger than $NO_3^-$ pool with lower $NO_3^-$ to
258 $NH_4^+$ ratios (< 0.2).
259 In MM area, needle $\delta^{15}N$ values were higher on the south-facing slope (+2.7‰ to
260 +4.3‰) where most sites were located in the boundary, than those on the
261 southwest-facing slope (+0.34‰ to +2.0‰) where all sites were located in the forest
262 (Figure 4(d)). In contrast, soil $\delta^{15}N$ slightly varied (+5.1 to +6.8‰) in MM area. The
263 $\Delta\delta^{15}N$ slightly changed from -4‰ to -2‰ at the sites on the south-facing slope, which
264 were smaller than those on the southwest-facing slope (-6‰) (Figure 4(e)). Needle $\delta^{13}C$
265 and needle N concentration were higher at the sites on the south-facing slope (-26.2‰
266 to -24.6‰) than those on the southwest-facing slope (-27.5‰ to -26.2‰) (Figure 4(f)).
267 KCl-extractable N (DON, $NH_4^+$, and $NO_3^-$) pools in the 0-20 cm soil layer were
268 observed at one forest site (MM3s) and three boundary sites (MM4s, MM5s, and
269 MM6s) on the south-facing slope in August 2012 (Table S1). The DON pool was more

than one-order of magnitude larger than $NH_4^+$ and $NO_3^-$ pools at all sites, just as observed in TR area. However, unlike forest sites in TR area, $NO_3^-$ pool size was similar to that of $NH_4^+$ at boundary sites (MM4s, MM5s, and MM6s), namely high $NO_3^-$ to $NH_4^+$ ratios (close to 1).

[Figure 4 near here]

### 3.4. *Relationships between $\delta^{15}N$ values and other parameters*

Significant correlations between different variables of all the sites in TR and MM areas were observed (Figure 5). The correlation was observed between needle $\delta^{13}C$ and needle $\delta^{15}N$ ($r_s = 0.877$) (Figure 5(a)), soil $\delta^{15}N$ and needle $\delta^{15}N$ ($r_s = 0.718$) (Figure 5(b)), needle N concentration and $\Delta\delta^{15}N$ ($r_s = 0.591$) (Figure 5(c)), and C/N ratio of bulk soil and $\Delta\delta^{15}N$ ($r_s = -0.541$) (Figure 5(d)). Data in MM area showed small $\Delta\delta^{15}N$ (-5‰ to -2‰), high needle $\delta^{15}N$ (+0.34‰ to +4.3‰), high soil $\delta^{15}N$ (+5.1‰ to +6.8‰), whereas in TR area showed larger variations in those values.

[Figure 5 near here]

## 4. Discussion

288 In this study, we observed large spatial variations in needle $\delta^{15}N$ and the difference
289 between needle and soil $\delta^{15}N$ ($\Delta\delta^{15}N$) at each area, whereas relatively small variation in
290 soil $\delta^{15}N$ (Figure 5(b)). The range of $\Delta\delta^{15}N$ observed in this study (6‰) (Figure 5(b))
291 accounts for a half of the global latitudinal variation [14], despite the same plant species
292 (*L. sibirica* Ledeb.), soil age, land use history, and climate. The spatial variation in
293 $\Delta\delta^{15}N$ indicates that the N cycle changes along the forest-grassland gradient. Here, the
294 isotope mass balance of available N in the soil was applied to understand the
295 mechanism of variation in $\Delta\delta^{15}N$.

296 First, we simplify the mass balance equations by deleting some terms in the equations
297 (1) and (2). Assuming a steady state condition of plant and soil N pools in the system,
298 the flux of input equals to that of loss ($F_{input} = F_{leach} + F_{gas}$), and then the equations (1)
299 and (2) can be simplified as follows:

300 $$F_a = F_p + F_m \quad (3)$$

301 $$\delta_a = \delta_s = f \times \delta_p + (1\text{-}f) \times \delta_m \quad (4)$$

302 where $\delta_s$ is soil $\delta^{15}N$, and f is the fraction of available N which is transported to the
303 plants ($f = F_p/F_a$). Namely, under a steady state condition, available N produced in the
304 soil is transported to plants and microorganisms. We assume that larch is the only plant
305 species (i.e. $\delta_p$ = needle $\delta^{15}N$), and also $\delta^{15}N$ of available N produced in the soil is the

306 same as that of the soil (i.e. $\delta_a = \delta_s$) as described in the Materials and methods. We focus
307 on the 0-20 cm soil layer to apply this mass balance, since all sites showed significant
308 increase in soil $\delta^{15}N$ at this layer (Figure 3), in which an active decomposition of soil
309 organic matter occurs [33].
310 From these equations, two processes could explain the small difference in $\delta^{15}N$
311 between larch needle and soil ($\Delta\delta^{15}N \cong 0$) observed at boundary sites (Figure 5(b)): (1)
312 available N is transported to larch and/or microorganisms without significant
313 fractionation ($\delta_a = \delta_p = \delta_m$), or (2) almost all available N is transported to larch ($f \cong 1$).
314 However, N immobilization by soil microorganisms ($F_m$) might not be a suitable
315 explanation, because it is generally accepted that immobilization is associated with
316 significant isotope fractionation, causing higher $\delta^{15}N$ in microorganisms than that of
317 substrate organic N [34,35]. Therefore, it is reasonable to consider that the observed
318 small $\Delta\delta^{15}N$ at boundary sites show that available N produced in the soil is mostly
319 transported to larch without significant fractionation. In contrast, large difference in
320 $\delta^{15}N$ between larch needle and soil ($\Delta\delta^{15}N < 0$) in forest sites (Figure 5(b)) suggests that
321 the $^{15}N$-depleted part of available N is transported to larch, whereas the$^{15}N$-enriched
322 part of available N is immobilized in soil microorganisms ($\delta_p < \delta_m$). This process is
323 consistent with previously observed $^{15}N$ enrichment in soil microorganisms during

immobilization [34,35], or with $^{15}N$ enrichment in the mycorrhizal fungal body and $^{15}N$-depletion in the host plant [36,37]. In fact, the observed magnitude of $\Delta\delta^{15}N$ at TR1n (8‰) was within the range of isotopic fractionation caused by ectomycorrhizal fungi (5‰ to 9‰) [38], although such large enrichment is not always observed [26]. Interpretations of $\Delta\delta^{15}N$ described above are also supported by other observed data. At boundary sites, a high needle N concentration, a low C/N ratio of bulk soil, and a high needle $\delta^{13}C$ were observed (Figure 5(a), 5(c), and 5(d)). Foliar N concentration and $\delta^{13}C$ have been frequently used as indicators of N availability for trees [39] and light and moisture conditions for plants [40], whereas the soil C/N as an indicator of the decomposition rate of soil organic matter [41]. Therefore, these parameters as well as the high $NO_3^-$ to $NH_4^+$ ratios at boundary sites in MM area (Table S1) indicate a rapid decomposition of soil organic matter and high N availability for larch under sunny and dry conditions. On the other hand, at forest sites forest, a low needle N concentration, a high C/N ratio of bulk soil, and a low needle $\delta^{13}C$ were observed (Figure 5(a), 5(c), and 5(d)), indicating the slow decomposition of soil organic matter and low N availability for larch under shady and relatively wet conditions. Our results suggest that the quantitative importance of the immobilization of available N, which is in agreement with a previous study that showed the severe competition of available N between plant

342 and soil microorganisms in taiga forest ecosystem [42].

343 In the mass balance equation, we assumed that the available N pool was theoretically
344 at a steady state condition. Strictly speaking, it is not always true, however, the input
345 and loss or their imbalance might not affect our interpretations described above.
346 Generally, recycled N within the plant-soil system provides the primary source of N for
347 biological activities in most terrestrial ecosystems [43]. Although there is not enough
348 data to evaluate the N budget at our study sites, we assume that recycled N is the
349 dominant flux compared with the input and loss fluxes in the plant-soil system. In taiga,
350 the annual N demand of larch has been reported at 1,500 mg N $m^{-2}$ $yr^{-1}$ near at Tura in
351 central Siberia [44], and 850 to 3,100 mg N $m^{-2}$ $yr^{-1}$ at Yakutsk in northeastern Siberia
352 [42]. The estimated N loss as leaching (< 10mg N $m^{-2}$ $yr^{-1}$) at Tura [44] and N input as
353 deposition (48 mg N $m^{-2}$ $yr^{-1}$) at Yakutsk [42] were much smaller than the N demand.

354 In TR area, N deposition has been observed to be 96 to 289 mg N $m^{-2}$ $yr^{-1}$ [45], much
355 smaller than the forest N demand estimated in central and northeastern Siberia.
356 Furthermore it is unlike that N deposition causes spatial variation in $\delta^{15}N$ observed at
357 such small spatial scale (less than 2 km) in each area, because the amount and isotopic
358 composition of N deposition may be similar at all sites in each area. Although an uptake
359 of atmospheric deposited N by forest canopy has been reported to be a significant N

360 source for trees in the region where atmospheric pollution is severe [46], it may not
361 affect our results for similar reasons described above.
362 Leaching ($F_{leach}$) seems to be insignificant in the boundary, since no runoff has been
363 reported at the grassland in TR area; whereas it may occur on the north-facing slope in
364 the forest [47]. However, leaching leads to loss of $^{15}N$-depleted N (such as $NO_3^-$), which
365 causes $^{15}N$ enrichment in available N especially inorganic N in the soil [48]. This
366 process is opposite to our interpretation to bear large $\Delta\delta^{15}N$ in the forest (i.e. larch
367 uptake $^{15}N$-depleted N which exists in the soil). The loss of N through $N_2O$ gas emission
368 seems to be very small, as shown in the temperate steppe (17 to 28 mg N $m^{-2}$ $yr^{-1}$) [49].
369 Therefore, both N input and loss processes may not be suitable to explain the variation
370 in $\Delta\delta^{15}N$ observed in this study.
371 In the above mass balance, we assumed that only the 0-20 cm soil layer provided
372 available N to larch; however, the organic layer may also provide available N [50]. The
373 organic layer showed lower $\delta^{15}N$ than the bulk soil (Figure 3), suggesting that the $\delta^{15}N$
374 of available N produced in the organic layer might be lower than that in the 0-20 cm soil
375 layer [51]. In the forest, where thick organic layer accumulates on the mineral soil layer,
376 larch uptake available N not only from the mineral soil layer, but also from the organic
377 layer; therefore, this additional uptake of lower $\delta^{15}N$ of available N from the organic

layer might contribute to large $\Delta\delta^{15}N$.

Recently, global syntheses of $\delta^{15}N$ values of plant and soil have been done by comparing the $\delta^{15}N$ data with climate variables such as mean annual temperature (MAT) and precipitation (MAP). Amundson et al. [14] compiled the $\delta^{15}N$ values from previous studies, performed regression analysis, and successfully formulated plant and soil $\delta^{15}N$ and their difference ($\Delta\delta^{15}N$) with MAT and MAP. In addition, Craine et al. [15] compiled foliar $\delta^{15}N$ and showed that foliar $\delta^{15}N$ increased with MAT at a rate of 0.23‰ $°C^{-1}$ for ecosystems with MAT > −0.5°C, and decreased by 2.6‰ for every order of magnitude increase of MAP. Similarly, Craine et al. [16] conducted an analysis with compiled soil $\delta^{15}N$, and reported that soil $\delta^{15}N$ increased with MAT at a rate of 0.18‰ $°C^{-1}$ for ecosystems with MAT > 9.8°C, showed no with MAT below 9.8°C, and decreased at a rate of 1.78‰ for every order of magnitude increase of MAP. Plant $\delta^{15}N$ values calculated for the MAT and MAP of TR and MM areas with the multi regression equation by Amundson et al. [14] derive -1.1‰ for TR area and -0.8‰ for MM area, and those values are close to the average for all sites in this study (+1.5 (±2.2)‰). Observed range in needle $\delta^{15}N$ (-3.9‰ to +4.3‰) also drops to the ranges of foliar $\delta^{15}N$ for both MAT and MAP as shown by Craine et al. [15]. Similarly, soil $\delta^{15}N$ values were calculated to be +3.2‰ and +3.4‰ with MAT and MAP for both TR and MM areas by

396 the multi regression equation [14], and these values are also close to the average for all
397 sites in this study (+5.2 (±1.0)‰). The observed range of soil $\delta^{15}N$ (+2.9‰ to +7.4‰) is
398 also within the range reported by Craine et al. [16]. It is worth noting that a large
399 difference in $\delta^{15}N$ values was observed between forest and boundary sites, but average
400 $\delta^{15}N$ values observed for all sites, nevertheless, are close to the values obtained from
401 global syntheses.

402 As described above, global distributions of foliar and soil $\delta^{15}N$, and their difference
403 ($\Delta\delta^{15}N$) depend on climate parameters [14–16]. The global map of $\Delta\delta^{15}N$ reported by
404 Amundson et al. [14] is therefore corresponding to the vegetation that also depends on
405 the climate [1]. $\Delta\delta^{15}N$ is larger in boreal forest and smaller in temperate grassland as
406 seen in their global map, and this trend is exactly consistent with this study. Here we
407 propose that the accumulation of organic layer, as a comprehensive process of N cycling
408 in the ecosystem, can be regarded as a key process which controls $\Delta\delta^{15}N$.

409

410

411 **5. Concluding remarks**

412 At a forest-grassland boundary in northern Mongolia, larch needle and soil $\delta^{15}N$ were
413 investigated to understand the mechanisms that control the spatial pattern of $\delta^{15}N$. The

414 difference between needle and soil $\delta^{15}N$ ($\Delta\delta^{15}N$) showed clear spatial variation along
415 the forest-grassland gradient with large $\Delta\delta^{15}N$ in the forest (up to -8‰) and small $\Delta\delta^{15}N$
416 in the grassland boundary (up to -2‰). The difference in $\delta^{15}N$ between larch and
417 mineral soil reflects the difference in the accumulation patterns of the organic layer. In
418 the grassland boundary, litter decomposes quickly and produced available N is
419 transported to larch without significant fractionation, whereas in the forest, larch trees
420 uptake available N with lower $\delta^{15}N$ than that produced in the soil. Namely, the
421 $^{15}N$-depleted part is taken by larch, whereas the $^{15}N$-enriched part remains in the soil,
422 which is balanced by $^{15}N$-depleted litter provided by larch. The divergence of available
423 N between larch and microorganisms in the soil, and the accumulation of diverged N in
424 the organic layer control the variation in $\Delta\delta^{15}N$.

425

426

427 **Acknowledgments**

428 We would like thank Drs. C. Mizota, S. Ishida, and F. Seidel for providing technical
429 information on sampling sites. We are also grateful to the members of the fieldwork
430 party in Mongolia for their support. We would also like to thank our lab staff and
431 colleagues for their support and valuable advice. This study was partly supported by the

Japan Society for the Promotion of Science with a Grant-in-Aid for Scientific Research (No. 26281003).

## References

[1] Ågren GI, Andersson FO. Terrestrial ecosystem ecology: principles and applications. Cambridge University Press; 2012.[2] Ometto J, Ehleringer JR, Domingues TF, Berry JA, Ishida FY, Mazzi E, et al. The stable carbon and nitrogen isotopic composition of vegetation in tropical forests of the Amazon Basin, Brazil. Biogeochemistry. 2006;79(1-2):251-74. doi: 10.1007/s10533-006-9008-8. PubMed PMID: WOS:000240033100013.

[3] Hogbom L, Nilsson U, Orlander G. Nitrate dynamics after clear felling monitored by in vivo nitrate reductase activity (NRA) and natural N-15 abundance of Deschampsia flexuosa (L.) Trin. Forest Ecology and Management. 2002;160(1-3):273-80. doi: 10.1016/s0378-1127(01)00475-3. PubMed PMID: WOS:000175374500023.

[4] Houlton BZ, Sigman DM, Hedin LO. Isotopic evidence for large gaseous nitrogen losses from tropical rainforests. Proceedings of the National Academy of Sciences of the United States of America. 2006;103(23):8745-50. doi: 10.1073/pnas.0510185103.

PubMed PMID: WOS:000238278400031.

[5] Frank DA, Groffman PM, Evans RD, Tracy BF. Ungulate stimulation of nitrogen cycling and retention in Yellowstone Park grasslands. Oecologia. 2000;123(1):116-21. doi: 10.1007/s004420050996. PubMed PMID: WOS:000086884300014.

[6] Hobbie EA, Macko SA, Williams M. Correlations between foliar delta N-15 and nitrogen concentrations may indicate plant-mycorrhizal interactions. Oecologia. 2000;122(2):273-83. doi: 10.1007/pl00008856. PubMed PMID: WOS:000085386700015.

[7] Evans RD. Physiological mechanisms influencing plant nitrogen isotope composition. Trends in Plant Science. 2001;6(3):121-6. doi: 10.1016/s1360-1385(01)01889-1. PubMed PMID: WOS:000167576600012.

[8] Zech M, Bimueller C, Hemp A, Samimi C, Broesike C, Hoerold C, et al. Human and climate impact on N-15 natural abundance of plants and soils in high-mountain ecosystems: a short review and two examples from the Eastern Pamirs and Mt. Kilimanjaro. Isotopes in Environmental and Health Studies. 2011;47(3):286-96. doi: 10.1080/10256016.2011.596277. PubMed PMID: WOS:000299723800006.

[9] Nadelhoffer KJ, Fry B. Nitrogen isotope studies in forest ecosystems. In : Lajtha K, Michener RH. Stable isotopes in ecology and environmental science. Blackwell

468 Scientific Publications; 1994. p. 22-44.

469 [10] Schulze ED, Chapin FS, Gebauer G. NITROGEN NUTRITION AND ISOTOPE

470 DIFFERENCES AMONG LIFE FORMS AT THE NORTHERN TREELINE OF

471 ALASKA. Oecologia. 1994;100(4):406-12. doi: 10.1007/bf00317862. PubMed PMID:

472 WOS:A1994QC13000008.

473 [11] Gebauer G, Giesemann A, Schulze ED, Jager HJ. ISOTOPE RATIOS AND

474 CONCENTRATIONS OF SULFUR AND NITROGEN IN NEEDLES AND SOILS OF

475 PICEA-ABIES STANDS AS INFLUENCED BY ATMOSPHERIC DEPOSITION OF

476 SULFUR AND NITROGEN-COMPOUNDS. Plant and Soil. 1994;164(2):267-81. doi:

477 10.1007/bf00010079. PubMed PMID: WOS:A1994PV72100013.

478 [12] Gebauer G, Schulze ED. CARBON AND NITROGEN ISOTOPE RATIOS IN

479 DIFFERENT COMPARTMENTS OF A HEALTHY AND A DECLINING

480 PICEA-ABIES FOREST IN THE FICHTELGEBIRGE, NE BAVARIA. Oecologia.

481 1991;87(2):198-207. doi: 10.1007/bf00325257. PubMed PMID:

482 WOS:A1991FX12200006.

483 [13] Jung K, Gebauer G, Gehre M, Hofmann D, Weissflog L, Schuurmann G.

484 Anthropogenic impacts on natural nitrogen isotope variations in Pinus sylvestris stands

485 in an industrially polluted area. Environmental Pollution. 1997;97(1-2):175-81. doi:

10.1016/s0269-7491(97)00053-5. PubMed PMID: WOS:A1997YD75800021.

[14] Amundson R, Austin AT, Schuur EAG, Yoo K, Matzek V, Kendall C, et al. Global patterns of the isotopic composition of soil and plant nitrogen. Global Biogeochemical Cycles. 2003;17(1). doi: 10.1029/2002gb001903. PubMed PMID: WOS:000182817800001.

[15] Craine JM, Elmore AJ, Aidar MPM, Bustamante M, Dawson TE, Hobbie EA, et al. Global patterns of foliar nitrogen isotopes and their relationships with climate, mycorrhizal fungi, foliar nutrient concentrations, and nitrogen availability. New Phytologist. 2009;183(4):980-92. doi: 10.1111/j.1469-8137.2009.02917.x. PubMed PMID: WOS:000268855300008.

[16] Craine JM, Elmore AJ, Wang LX, Augusto L, Baisden WT, Brookshire ENJ, et al. Convergence of soil nitrogen isotopes across global climate gradients. Scientific Reports. 2015;5. doi: 10.1038/srep08280. PubMed PMID: WOS:000348903800001.

[17] Pardo LH, Hemond HF, Montoya JP, Pett-Ridge J. Natural abundance N-15 in soil and litter across a nitrate-output gradient in New Hampshire. Forest Ecology and Management. 2007;251(3):217-30. doi: 10.1016/j.foreco.2007.06.047. PubMed PMID: WOS:000250743000009.

[18] Garten CT, Vanmiegroet H. RELATIONSHIPS BETWEEN SOIL-NITROGEN

504 DYNAMICS AND NATURAL N-15 ABUNDANCE IN PLANT FOLIAGE FROM
505 GREAT SMOKY MOUNTAINS NATIONAL-PARK. Canadian Journal of Forest
506 Research-Revue Canadienne De Recherche Forestiere. 1994;24(8):1636-45. doi:
507 10.1139/x94-212. PubMed PMID: WOS:A1994QA52700014.
508 [19] Brenner DL, Amundson R, Baisden WT, Kendall C, Harden J. Soil N and N-15
509 variation with time in a California annual grassland ecosystem. Geochimica Et
510 Cosmochimica Acta. 2001;65(22):4171-86. doi: 10.1016/s0016-7037(01)00699-8.
511 PubMed PMID: WOS:000172349700007.
512 [20] Averill C, Finzi AC. Increasing plant use of organic nitrogen with elevation is
513 reflected in nitrogen uptake rates and ecosystem delta N-15. Ecology.
514 2011;92(4):883-91. doi: 10.1890/10-0746.1. PubMed PMID: WOS:000290533700010.
515 [21] Callesen I, Nilsson LO, Schmidt IK, Vesterdal L, Ambus P, Christiansen JR, et al.
516 The natural abundance of N-15 in litter and soil profiles under six temperate tree
517 species: N cycling depends on tree species traits and site fertility. Plant and Soil.
518 2013;368(1-2):375-92. doi: 10.1007/s11104-012-1515-x. PubMed PMID:
519 WOS:000321641700028.
520 [22] Brearley FQ. Nitrogen stable isotopes indicate differences in nitrogen cycling
521 between two contrasting Jamaican montane forests. Plant and Soil.

2013;367(1-2):465-76. doi: 10.1007/s11104-012-1469-z. PubMed PMID: WOS:000319771700033.

[23] Emmett BA, Kjonaas OJ, Gundersen P, Koopmans C, Tietema A, Sleep D. Natural abundance of N-15 in forests across a nitrogen deposition gradient. Forest Ecology and Management. 1998;101(1-3):9-18. doi: 10.1016/s0378-1127(97)00121-7. PubMed PMID: WOS:000072095800002.

[24] Schuur EAG, Matson PA. Net primary productivity and nutrient cycling across a mesic to wet precipitation gradient in Hawaiian montane forest. Oecologia. 2001;128(3):431-42. doi: 10.1007/s004420100671. PubMed PMID: WOS:000170499400015.

[25] Hobbie EA, Macko SA, Shugart HH. Insights into nitrogen and carbon dynamics of ectomycorrhizal and saprotrophic fungi from isotopic evidence. Oecologia. 1999;118(3):353-60. doi: 10.1007/s004420050736. PubMed PMID: WOS:000079391900009.

[26] Gebauer G, Meyer M. N-15 and C-13 natural abundance of autotrophic and mycoheterotrophic orchids provides insight into nitrogen and carbon gain from fungal association. New Phytologist. 2003;160(1):209-23. doi: 10.1046/j.1469-8137.2003.00872.x. PubMed PMID: WOS:000185557300024.

[27] Garten CT. VARIATION IN FOLIAR N-15 ABUNDANCE AND THE AVAILABILITY OF SOIL-NITROGEN ON WALKER BRANCH WATERSHED. Ecology. 1993;74(7):2098-113. doi: 10.2307/1940855. PubMed PMID: WOS:A1993LY54900021.

[28] Li SG, Asanuma J, Kotani A, Eugster W, Davaa G, Oyunbaatar D, Sugita M. Year-round measurements of net ecosystem CO2 flux over a montane larch forest in Mongolia. Journal of Geophysical Research-Atmospheres 110. 2005. doi: 10.1029/2004jd005453

[29] Ishikawa M, Sharkuu N, Zhang YS, Kadota T, Ohata TT. Ground thermal and moisture conditions at the southern boundary of discontinuous permafrost, Mongolia. Permafrost and Periglacial Processes. 2005;16(2):209-16. doi: 10.1002/ppp.483. PubMed PMID: WOS:000229979600006.

[30] Peel MC, Finlayson BL, McMahon TA. Updated world map of the Koppen-Geiger climate classification. Hydrology and Earth System Sciences. 2007;11(5):1633-44. PubMed PMID: WOS:000251516100009.

[31] Tuhkanen S. Treeline in relation to climate, with special reference to oceanic areas. In : Alden JN, Mastrantonio JL, Ødum S. Forest development in cold climates. Springer US; 1993. p. 115-134.

558 [32] Ponge JF. Humus forms in terrestrial ecosystems: a framework to biodiversity. Soil
559 Biology & Biochemistry. 2003;35(7):935-45. doi: 10.1016/s0038-0717(03)00149-4.
560 PubMed PMID: WOS:000184125500007.
561 [33] Hobbie EA, Ouimette AP. Controls of nitrogen isotope patterns in soil profiles.
562 Biogeochemistry. 2009;95(2-3):355-71. doi: 10.1007/s10533-009-9328-6. PubMed
563 PMID: WOS:000269837900012.
564 [34] Dijkstra P, LaViolette CM, Coyle JS, Doucett RR, Schwartz E, Hart SC, et al. N-15
565 enrichment as an integrator of the effects of C and N on microbial metabolism and
566 ecosystem function. Ecology Letters. 2008;11(4):389-97. doi:
567 10.1111/j.1461-0248.2008.01154.x. PubMed PMID: WOS:000254628000010.
568 [35] Coyle JS, Dijkstra P, Doucett RR, Schwartz E, Hart SC, Hungate BA.
569 Relationships between C and N availability, substrate age, and natural abundance C-13
570 and N-15 signatures of soil microbial biomass in a semiarid climate. Soil Biology &
571 Biochemistry. 2009;41(8):1605-11. doi: 10.1016/j.soilbio.2009.04.022. PubMed PMID:
572 WOS:000268920400003.
573 [36] Gebauer G, Dietrich P. Nitrogen isotope ratios in different compartments of a
574 mixed stand of spruce, larch and beech trees and of understory vegetation including
575 fungi. Isotopes in Environmental and Health Studies. 1993;29(1-2):35-44. doi:

576 10.1080/10256019308046133.

577 [37] Michelsen A, Quarmby C, Sleep D, Jonasson S. Vascular plant N-15 natural

578 abundance in heath and forest tundra ecosystems is closely correlated with presence and

579 type of mycorrhizal fungi in roots. Oecologia. 1998;115(3):406-18. doi:

580 10.1007/s004420050535. PubMed PMID: WOS:000074877400017.

581 [38] Hobbie EA, Hogberg P. Nitrogen isotopes link mycorrhizal fungi and plants to

582 nitrogen dynamics. New Phytologist. 2012;196(2):367-82. doi:

583 10.1111/j.1469-8137.2012.04300.x. PubMed PMID: WOS:000308882200009. [39]

584 Liang MC, Sugimoto A, Tei S, Bragin IV, Takano S, Morozumi T, et al. Importance of

585 soil moisture and N availability to larch growth and distribution in the Arctic

586 taiga-tundra boundary ecosystem, northeastern Siberia. Polar Science. 2014;8(4):327-41.

587 doi: 10.1016/j.polar.2014.07.008. PubMed PMID: WOS:000346894800002.

588 [40] Farquhar GD, Ehleringer JR, Hubick KT. CARBON ISOTOPE

589 DISCRIMINATION AND PHOTOSYNTHESIS. Annual Review of Plant Physiology

590 and Plant Molecular Biology. 1989;40:503-37. doi: 10.1146/annurev.arplant.40.1.503.

591 PubMed PMID: WOS:A1989U857900019.

592 [41] Finzi AC, Van Breemen N, Canham CD. Canopy tree soil interactions within

593 temperate forests: Species effects on soil carbon and nitrogen. Ecological Applications.

1998;8(2):440-6. doi: 10.2307/2641083. PubMed PMID: WOS:000073447900023.

[42] Popova AS, Tokuchi N, Ohte N, Ueda MU, Osaka K, Maximov TC, et al. Nitrogen availability in the taiga forest ecosystem of northeastern Siberia. Soil Science and Plant Nutrition. 2013;59(3):427-41. doi: 10.1080/00380768.2013.772495. PubMed PMID: WOS:000322809800014.

[43] Parton W, Silver WL, Burke IC, Grassens L, Harmon ME, Currie WS, et al. Global-scale similarities in nitrogen release patterns during long-term decomposition. Science. 2007;315(5810):361-4. doi: 10.1126/science.1134853. PubMed PMID: WOS:000243535400037.

[44] Tokuchi N, Hirobe M, Kondo K, Arai H, Hobara S, Fukushima K, Matsuura Y. Permafrost Ecosystems: Siberian Larch Forests. Springer: Netherlands; 2010. Soil nitrogen dynamics in larch ecosystem; p. 229–243.

[45] EANET Data on the Acid Deposition in the East Asian Region (2002-2011) [Internet]. Network Center for EANET. Available from: http://www.eanet.asia/index.html

[46] Harrison AF, Schulze ED, Gebauer G, et al. Canopy uptake and utilization of atmospheric pollutant nitrogen. In : Schulze ED. Carbon and nitrogen cycling in European forest ecosystems. Springer-Verlag Berlin Heidelberg; 2000. p. 171-188.

612 [47] Iijima Y, Ishikawa M, Jambaljav Y. Hydrological cycle in relation to permafrost
613 environment in forest-grassland ecotone in Mongolia. Journal of Japanese Association
614 of Hydrological Sciences. 2012;42:119-130.
615 [48] Martinelli LA, Piccolo MC, Townsend AR, Vitousek PM, Cuevas E, McDowell W,
616 et al. Nitrogen stable isotopic composition of leaves and soil: Tropical versus temperate
617 forests. Biogeochemistry. 1999;46(1-3):45-65. doi: 10.1023/a:1006100128782. PubMed
618 PMID: WOS:000080776300004.
619 [49] Wolf B, Zheng XH, Brueggemann N, Chen WW, Dannenmann M, Han XG, et al.
620 Grazing-induced reduction of natural nitrous oxide release from continental steppe.
621 Nature. 2010;464(7290):881-4. doi: 10.1038/nature08931. PubMed PMID:
622 WOS:000276397300035.
623 [50] Tietema A, Warmerdam B, Lenting E, Riemer L. ABIOTIC FACTORS
624 REGULATING NITROGEN TRANSFORMATIONS IN THE ORGANIC LAYER OF
625 ACID FOREST SOILS - MOISTURE AND PH. Plant and Soil. 1992;147(1):69-78.
626 doi: 10.1007/bf00009372. PubMed PMID: WOS:A1992KK11100008.
627 [51] Koba K, Hirobe M, Koyama L, Kohzu A, Tokuchi N, Nadelhoffer KJ, et al. Natural
628 N-15 abundance of plants and soil N in a temperate coniferous forest. Ecosystems.
629 2003;6(5):457-69. doi: 10.1007/s10021-002-0132-6. PubMed PMID:

630 WOS:000185256000005.

631

632

633

634

635

636

637

638

639

640

641

642

643

644

645

646 Table 1. Locations of sampling sites.

| Area name | code | Site No.[a] position | Latitude °N | Longitude °E | Elevation m |
|---|---|---|---|---|---|
| Terelj | TR | 1n, 2n, 3n, 4n, 5n, 6n, 7n, 8n | 47.97 | 107.42 | 1587-1750 |
| | | ic | 47.98 | 107.40 | 1639 |
| | | 1s, 2s | 47.99 | 107.42 | 1651-1791 |
| Mongonmorit | MM | 1s, 2s, 3s, 4s, 5s, 6s, 7s | 48.35 | 108.66 | 1525-1619 |
| | | 1sw, 2sw, 3sw | 48.35 | 108.65 | 1593-1623 |

647

648 [a] Each sampling site is expressed by area code and position on a slope. The position

649 number increases along upper to lower slope. The letter after position number indicates

650 the direction of slope. For example, “n” means north-facing slope and “sw” means

651 southwest-facing slope. TRic is a site in valley.

652

653

654

655

656

657

658

659

660 Figure 1. A map of the two observation areas (TR and MM) and Ulaanbaatar, the capital
661 of Mongolia (a), and schematic figures of longitudinal cross sections in TR area (b) and
662 MM area (c). Samplings were conducted at Terelj (TR) and Mongonmorit (MM) at the
663 forest-grassland boundary in northern Mongolia. In TR area, sampling was conducted at
664 11 sites along a transect line from the north-facing slope to the south-facing slope over a
665 valley. In MM area, two transects were set on the south-facing slope and the
666 southwest-facing slope, and sampling was conducted at 10 sites.
667
668 Figure 2. Temporal variations in larch needle N concentration (a), $\delta^{15}N$ (b), and $\delta^{13}C$ (c)
669 in TR area. Data from two trees at TR3n, four trees at TR6n, and three trees at TR1s are
670 shown. Each tree is expressed by a different shape (circle, rectangle, or triangle) and
671 colour (black or white). Trees within the same site share the same shape.
672
673 Figure 3. Vertical profiles of larch needle, organic layer, and bulk soil $\delta^{15}N$ values at the
674 forest site (TR1n) and the boundary site (TR7n) in TR area. Bars represent standard
675 deviation of the mean.
676
677 Figure 4. Spatial variations in larch needle (triangle) and soil (square) $\delta^{15}N$ (a),

678 differences in $\delta^{15}N$ between needle and soil ($\Delta\delta^{15}N$) (b), and needle $\delta^{13}C$ (open-triangle)

679 and N concentration (filled-triangle) (c) in TR area, and the same as (d), (e), and (f) in

680 MM area. Bars represent standard deviation of the mean.

681

682 Figure 5. Correlations between larch needle $\delta^{13}C$ and $\delta^{15}N$ ($r_s = 0.877$) (a), needle and

683 soil $\delta^{15}N$ ($r_s = 0.718$) (b), needle N concentration and $\Delta\delta^{15}N$ ($r_s = 0.591$) (c), and C/N

684 ratio of bulk soil and $\Delta\delta^{15}N$ ($r_s = -0.541$) (d) at all sites in TR area (circle) and MM area

685 (triangle). Dotted lines in (b) indicate $\Delta\delta^{15}N$ values at 0‰, -4‰ and -8‰. Correlation

686 coefficients are significant at $p < 0.05$. Bars represent standard deviation of the mean.

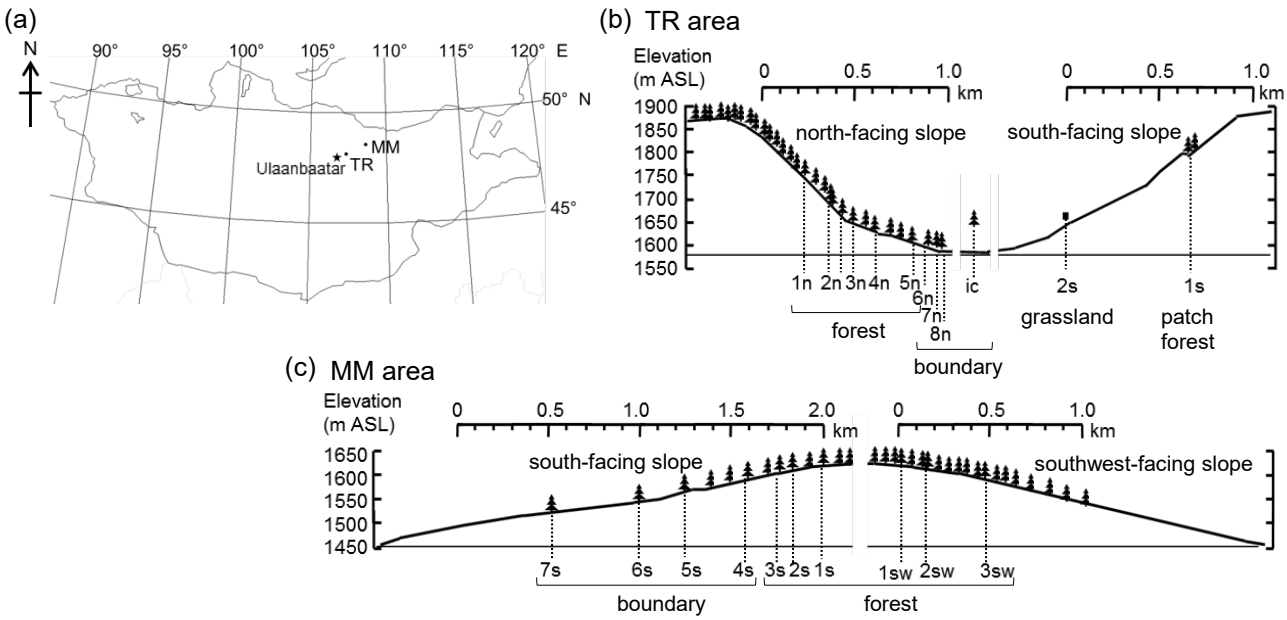


**Figure 1.**

A map of the two observation areas (TR and MM) and Ulaanbaatar, the capital of Mongolia (a), and schematic figures of longitudinal cross sections in TR area (b) and MM area (c). Samplings were conducted at Terelj (TR) and Mongonmorit (MM) at the forest-grassland boundary in northern Mongolia. In TR area, sampling was conducted at 11 sites along a transect line from the north-facing slope to the south-facing slope over a valley. In MM area, two transects were set on the south-facing slope and the southwest-facing slope, and sampling was conducted at 10 sites.

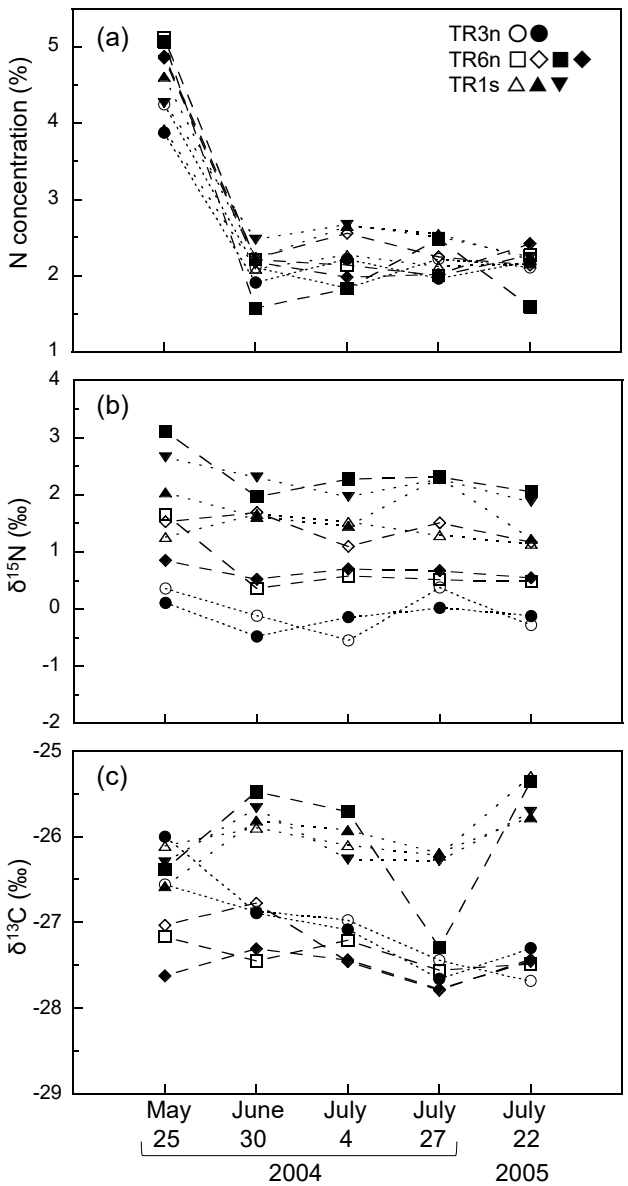


**Figure 2.**

Temporal variations in larch needle N concentration (a), $\delta^{15}N$ (b), and $\delta^{13}C$ (c) in TR area. Data from two trees at TR3n, four trees at TR6n, and three trees at TR1s are shown. Each tree is expressed by a different shape (circle, rectangle, or triangle) and colour (black or white). Trees within the same site share the same shape.

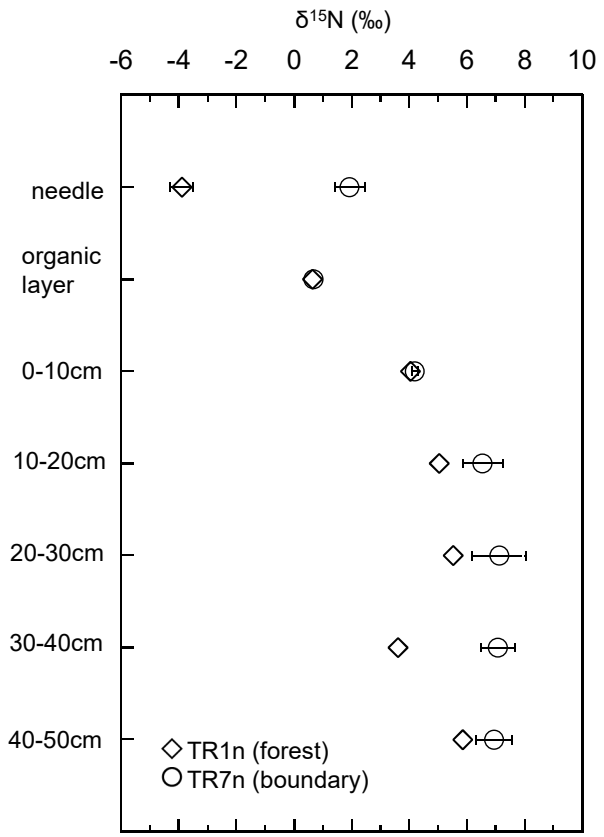


**Figure 3.**

Vertical profiles of larch needle, organic layer, and bulk soil $\delta^{15}N$ values at the forest site (TR1n) and the boundary site (TR7n) in TR area. Bars represent standard deviation of the mean.

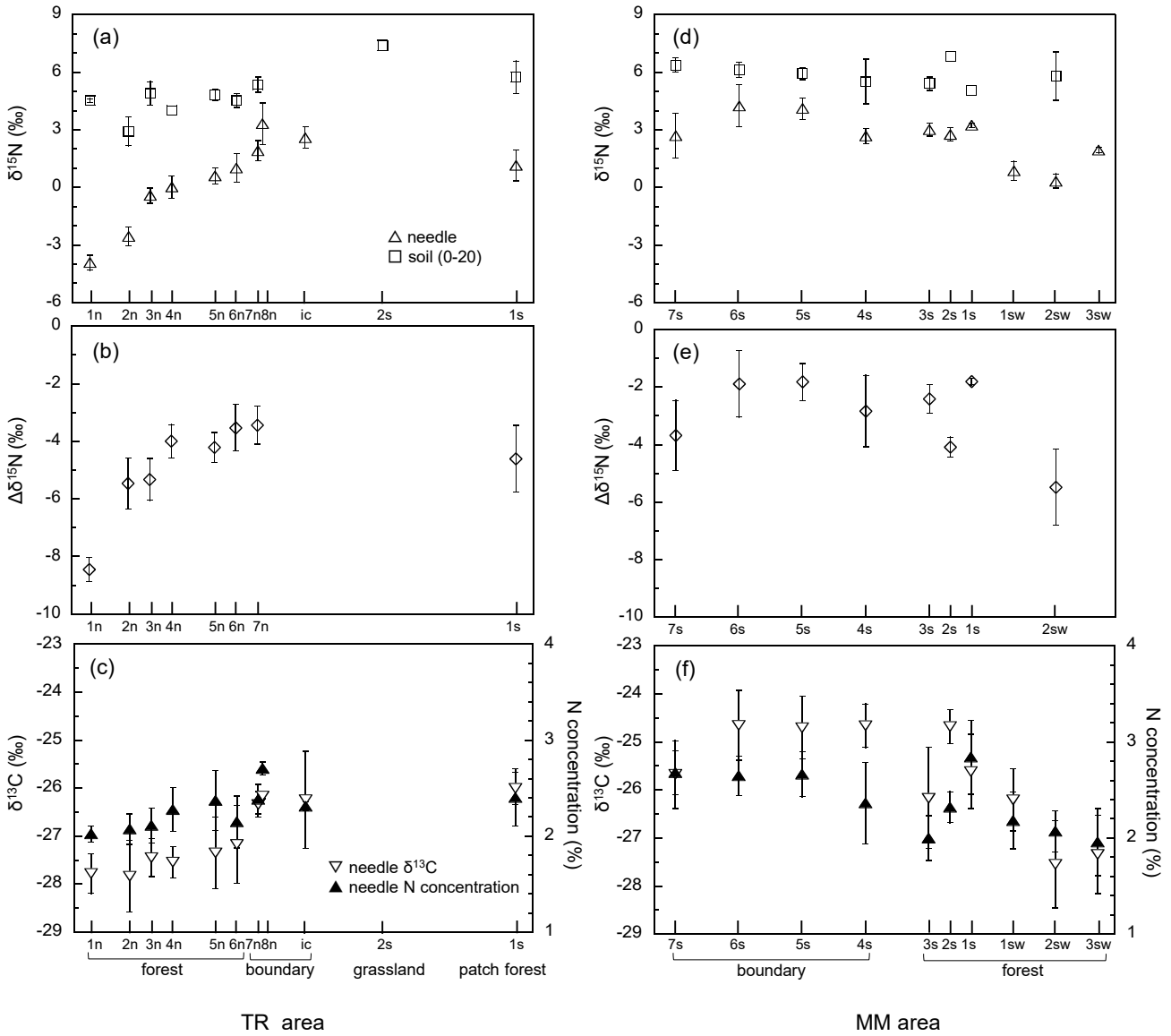


**Figure 4.**

Spatial variations in larch needle (triangle) and soil (square) $\delta^{15}N$ (a), differences in $\delta^{15}N$ between needle and soil ($\Delta\delta^{15}N$) (b), and needle $\delta^{13}C$ (open-triangle) and N concentration (filled-triangle) (c) in TR area, and the same as (d), (e), and (f) in MM area. Bars represent standard deviation of the mean.

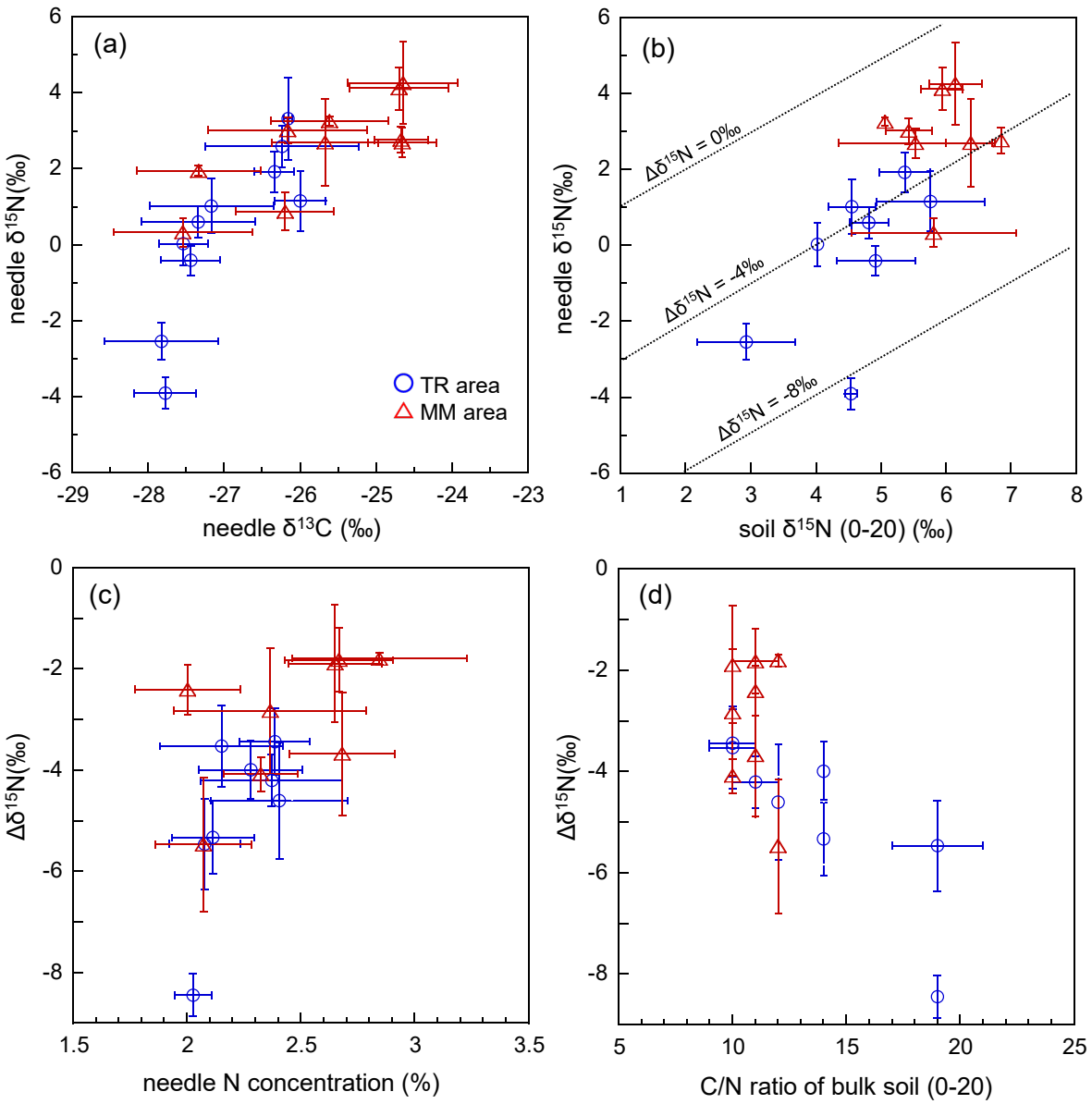


**Figure 5.**

Correlations between larch needle $\delta^{13}C$ and $\delta^{15}N$ ($r_s = 0.877$) (a), needle and soil $\delta^{15}N$ ($r_s = 0.718$) (b), needle N concentration and $\Delta\delta^{15}N$ ($r_s = 0.591$) (c), and C/N ratio of bulk soil and $\Delta\delta^{15}N$ ($r_s = -0.541$) (d) at all sites in TR area (circle) and MM area (triangle). Dotted lines in (b) indicate $\Delta\delta^{15}N$ values at 0‰, -4‰ and -8‰. Correlation coefficients are significant at $p < 0.05$. Bars represent standard deviation of the mean.

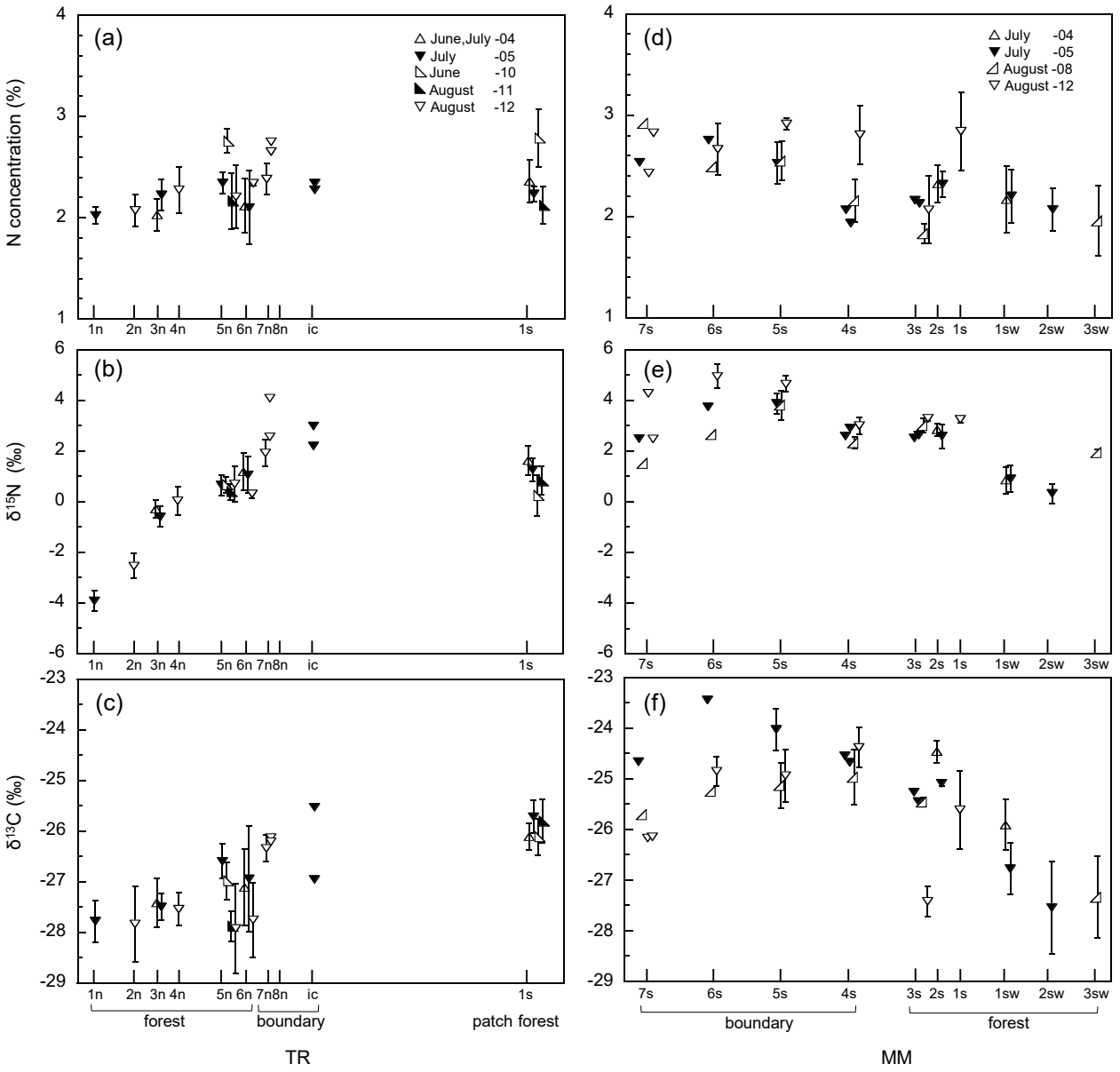


**Figure S1.**
Larch needle N concentration (a), $\delta^{15}N$ (b), and $\delta^{13}C$ (c) in TR area, and the same as (d), (e), and (f) in MM area observed on all sampling dates at each site . Bars represent standard deviation of the mean.

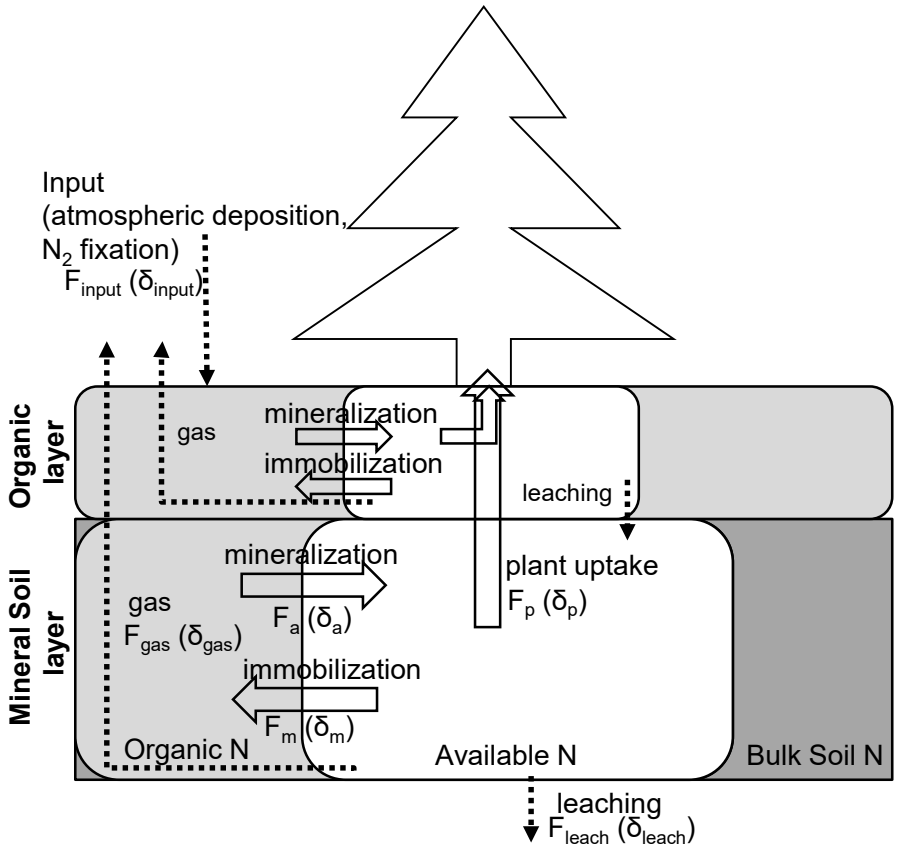


**Figure S2.**
The schematic representation of mass balance of biologically available N in plant-soil system.
Assuming that the available N pool is at a steady state, the following equations are established:

$$F_{input} + F_a = F_p + F_m + F_{leach} + F_{gas} \quad (1)$$

and for $\delta^{15}N$,

$$F_{input} \times \delta_{input} + F_a \times \delta_a = F_p \times \delta_p + F_m \times \delta_m + F_{leach} \times \delta_{leach} + F_{gas} \times \delta_{gas} \quad (2)$$

where $F_{input}$ is the N derived from atmospheric N deposition and biological $N_2$ fixation, and $F_a$ is the N produced in the soil through the decomposition of soil organic matter. $F_P$ and $F_m$ are the fluxes of available N taken up by plants and immobilized by soil microorganisms, respectively. $F_{leach}$ and $F_{gas}$ are the N lost due to leaching and gaseous emission, respectively. The values of $\delta_{input}$, $\delta_a$, $\delta_{p,}$ $\delta_m$, $\delta_{leach}$, and $\delta_{gas}$ are the $\delta^{15}N$ of input, produced N from soil organic matter, plant uptake, immobilization by soil microorganisms, leaching, and gaseous emission of available N, respectively. We assumed that larch was the only plant species (i.e. $\delta_p$ = needle $\delta^{15}N$), and that the $\delta^{15}N$ of available N produced in the soil was the same as that of the soil (i.e. $\delta_a$ = soil $\delta^{15}N$).